MAPK inhibitors, particularly the JNK inhibitor, increase cell death effects in H_2O_2-treated lung cancer cells via increased superoxide anion and glutathione depletion

WOO HYUN PARK

Department of Physiology, Medical School, Research Institute for Endocrine Sciences, Chonbuk National University, Jeonju, Jeollabuk-do 54907, Republic of Korea

Abstract. Reactive oxygen species (ROS), especially hydrogen peroxide (H_2O_2), induce apoptosis in cancer cells by regulating mitogen-activated protein kinase (MAPK) signaling pathways. The present study investigated the effects of MAPK inhibitors on cell growth and death as well as changes in ROS and glutathione (GSH) levels in H_2O_2-treated Calu-6 and A549 lung cancer cells. H_2O_2 inhibited growth and induced death of Calu-6 and A549 lung cancer cells. All MAPK inhibitors appeared to enhance growth inhibition in H_2O_2-treated Calu-6 and A549 lung cancer cells and increased the percentage of Annexin V-FITC-positive cells in these cancer cells. Among the MAPK inhibitors, a JNK inhibitor significantly augmented the loss of mitochondrial membrane potential (MMP; $\Delta\Psi_m$) in H_2O_2-treated Calu-6 and A549 lung cancer cells. Intracellular ROS levels were significantly increased in the H_2O_2-treated cells at 1 and 24 h. Only the JNK inhibitor increased ROS levels in the H_2O_2-treated cells at 1 h and all MAPK inhibitors raised superoxide anion levels in these cells at 24 h. In addition, H_2O_2 induced GSH depletion in Calu-6 and A549 cells and the JNK inhibitor significantly enhanced GSH depletion in H_2O_2-treated cells. Each of the MAPK inhibitors altered ROS and GSH levels differently in the Calu-6 and A549 control cells. In conclusion, H_2O_2 induced growth inhibition and death in lung cancer cells through oxidative stress and depletion of GSH. The enhanced effect of MAPK inhibitors, especially the JNK inhibitor, on cell death in H_2O_2-treated lung cancer cells was correlated with increased $O_2\cdot^-$ levels and GSH depletion.

Introduction

Superoxide anion ($O_2\cdot^-$), hydroxyl radical ($\cdot OH$) and hydrogen peroxide (H_2O_2) are unstable and highly reactive oxygen species (ROS). Although ROS are conventionally harmful or detrimental to cells, they specifically regulate a variety of cellular procedures such as cell proliferation, differentiation and apoptosis (1,2). ROS are persistently produced during the respiratory chain reaction during oxidative phosphorylation in the form of $O_2\cdot^-$ and/or are intentionally generated by specific oxidase enzymes (3). $O_2\cdot^-$ is converted into H_2O_2 by superoxide dismutase (4). H_2O_2 is further metabolized into O_2 and H_2O by catalase or glutathione (GSH) peroxidase (5). Compared to other types of ROS, H_2O_2 is nonradical and soluble in both lipid and aqueous surroundings. It freely diffuses all the way through the cell membrane to reach remote cells and interacts with ferrous iron (Fenton reaction), resulting in the generation of the tremendously violent and short-lived $\cdot OH$. Since the production of different forms of ROS at numerous levels can be either useful or harmful to cells and tissues, a redox state is steadfastly controlled to avoid cell and tissue damage. Enhanced oxidative stress as a consequence of either overproduction of ROS and/or downregulation of antioxidants leads to apoptotic cell death via injury to cellular DNA, proteins and lipids and is associated with a variety of pathological conditions such as inflammation and immune responses (6,7).

Mitogen-activated protein kinases (MAPKs) are evolutionarily conserved signaling proteins that mediate responses to assorted stimuli. Extracellular signal regulated kinases (ERK1/2), the c-Jun N-terminal kinase/stress-activated protein kinases (JNK/SAPK) and the p38 kinases are the three main MAPK groups in mammalians/eukaryotes (8). Each MAPK pathway has comparatively unrelated upstream activators and specific substrates (9). The trigger for multiple MAPK

Correspondence to: Professor Woo Hyun Park, Department of Physiology, Medical School, Research Institute for Endocrine Sciences, Chonbuk National University, 20 Geonji-ro, Deokjin-gu, Jeonju, Jeollabuk-do 54907, Republic of Korea
E-mail: parkwh71@jbnu.ac.kr

pathways includes major constituents of signaling pathways in cell growth, cell death and differentiation (10). MAPKs can discriminate the cellular redox status and are common targets for ROS themselves. For instance, JNK and p38 are normally activated by a soft oxidative stress and their activation induces apoptosis in cells (11,12). Furthermore, ROS can stimulate the ERK pathway by specific phosphorylation of the ERK enzyme (13). As a general rule, the activation of ERK is involved in cell survival rather than cell death (14). In addition, the activity of MAPKs is persistent by means of the subordinate activity of MAPK phosphatases, which are directly controlled by H$_2$O$_2$ (15).

Lung cancer is a major cause of cancer-related mortality in developed countries. The carcinogenesis of lung cancer is closely related to tissue inflammation mediated by ROS. During inflammation, the concentration of H$_2$O$_2$ in tissues is anticipated to reach approximately millimolar levels (16,17). Moderate H$_2$O$_2$ levels may adjust important cellular events, such as cell growth and differentiation, by altering signaling cascades and gene expression and its upper levels can elicit cell death via apoptosis or necrosis. The lung is particularly prone to an assortment of blood- and air-borne damage, which may consequently induce lung fibrosis and cancer (18). Exogenous H$_2$O$_2$ is frequently used to provoke oxidative stress in cells and tissues. Because different ROS levels and cellular roles of MAPKs modulated by ROS may have opposing properties, even within the same cell type, the relationship between ROS and MAPK signaling with respect to cell growth and death needs to be further clarified. Using specific MAPK inhibitors [JNK inhibitor (SP600125), MEK inhibitor (PD98059) and p38 inhibitor (SB203580)], the present study sought to elucidate the roles of different MAPKs in H$_2$O$_2$-treated Calu-6 and A549 lung cancer cells in relation to cell growth and death as well as investigate changes in ROS and GSH levels.

Materials and methods

Cell culture. The human lung cancer cell lines, Calu-6 and A549, were obtained from the Korean Cell Line Bank (Seoul, Korea) and cultured in RPMI-1640 medium (GE Healthcare Life Sciences, Logan, UT, USA) with 10% fetal bovine serum (FBS; Sigma-Aldrich; Merck KGaAA, Darmstadt, Germany) and 1% penicillin-streptomycin (Gibco; Thermo Fisher Scientific, Inc., Waltham, MA, USA). The cells were routinely cultivated in 100-mm plastic tissue culture dishes (Nalge Nunc International, Penfield, NY, USA) in a humidified incubator containing 5% CO$_2$, at 37°C and harvested in a solution of trypsin-EDTA (Gibco; Thermo Fisher Scientific, Inc.) while in a logarithmic phase of growth.

Reagents. H$_2$O$_2$ was purchased from Sigma-Aldrich; Merck KGaAA. The MEK inhibitor (PD98059) as well as the JNK (SP600125) and p38 (SB203580) inhibitors were obtained from Calbiochem (San Diego, CA, USA). All reagents were dissolved in dimethyl sulfoxide (DMSO; Sigma-Aldrich; Merck KGaAA) at 10 mM. The cells were pretreated with each MAPK inhibitor for 30 min prior to treatment with H$_2$O$_2$. Based on previous experiments (19-21), 10 μM of each MAPK inhibitor was applied as an optimal dose in all experiments.

Cell growth assay. The effect of the drugs on lung cancer cell growth was determined by evaluating 3-(4,5-dimethylthiazol-2-yl)-2,5-diphenyltetrazolium bromide (MTT; Sigma-Aldrich; Merck KGaAA) dye absorbance as previously described (19-21). The cells were exposed to 75 or 100 μM H$_2$O$_2$ with or without 10 μM MEK, JNK or p38 inhibitor for 24 h.

Sub-G1 cell analysis. Sub-G1 cells were detected using propidium iodide dye (PI; Sigma-Aldrich; Merck KGaA) as previously described (20,21). The cells were exposed to 75 or 100 μM H$_2$O$_2$ in the presence or absence of 10 μM MEK, JNK or p38 inhibitor for 24 h. The cell DNA content was assessed by a FACStar flow cytometer (BD Biosciences, Franklin Lakes, NJ, USA) and analyzed using Lysis II and Cellfit software version 2.0 (BD Biosciences).

Annexin V staining for cell death detection. Apoptotic cell death was evaluated by measuring cell stained with Annexin V-fluorescein isothiocyanate (FITC; Molecular Probes; Thermo Fisher Scientific, Inc.) as previously described (19-21). The cells were exposed to 75 or 100 μM H$_2$O$_2$ with or without 10 μM MEK, JNK, or p38 inhibitor for 24 h. Annexin V staining was analyzed with a FACStar flow cytometer (BD Biosciences).

Measurement of mitochondrial membrane potential (MMP; $\Delta\Psi_m$). MMP was assessed using Rhodamine 123 mitochondrial-specific fluorescent dye (Sigma-Aldrich; Merck KGaAA) as previously described (19-21). The cells were exposed to 75 or 100 μM H$_2$O$_2$ in the presence or absence of 10 μM MEK, JNK, or p38 inhibitor for 24 h. Rhodamine 123 staining intensity was assessed by a FACStar flow cytometer (BD Biosciences). An absence of Rhodamine 123 from the cells indicated a loss of MMP in lung cancer cells. Similarly to previous experiments (19-21), the MMP levels in the cells excluding MMP-loss cells were expressed as the mean fluorescence intensity (MFI), which was estimated by CellQuest Pro software (version 5.1; BD Biosciences).

Measurement of intracellular ROS levels. The intracellular ROS levels were evaluated by a fluorescent probe dye, 2',7'-dichlorodihydrofluorescein diacetate (H$_2$DCFDA; Molecular Probes; Thermo Fisher Scientific, Inc.) at 1 or 24 h as previously described (19-21). Dihydroethidium (DHE; Molecular Probes; Thermo Fisher Scientific, Inc.) is a fluorogenic probe specific to O$_2$·- in ROS. In brief, the cells were treated with 75 or 100 μM H$_2$O$_2$ in the presence or absence of 10 μM MEK, JNK or p38 inhibitor in the presence of 20 μM H$_2$DCFDA or DHE. The levels of DCF (ROS) and DHE (O$_2$·-) fluorescence were assessed using a FACStar flow cytometer (BD Biosciences) at 1 h and expressed as MFI, as calculated by CellQuest Pro software (version 5.1; BD Biosciences). Additionally, the cells were incubated with 75 or 100 μM H$_2$O$_2$ in the presence or absence of each MAPK inhibitor for 24 h. The cells were incubated with 20 μM H$_2$DCFDA or DHE at 37°C for 30 min. H$_2$DCFDA and DHE fluorescence was analyzed using a FACStar flow cytometer (BD Biosciences).

Detection of intracellular GSH. The GSH levels were evaluated by means of a 5-chloromethylfluorescein diacetate dye
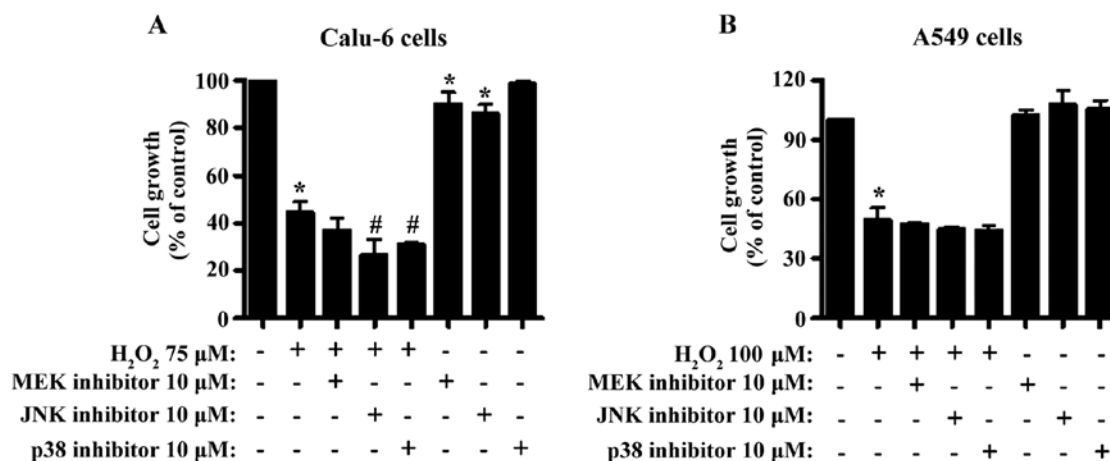
Figure 1. Effects of MAPK inhibitors on cell growth in H_2O_2-treated lung cancer cells. After 30 min of preincubation with the respective MAPK inhibitors, the exponentially growing lung cancer cells were treated with 75 or 100 μM H_2O_2 for 24 h. (A and B) The graphs demonstrate the growth changes in Calu-6 and A549 cells, as assessed by MTT assays. *P<0.05 compared to the control group. #P<0.05 compared to cells treated only with H_2O_2.

(CMFDA; Molecular Probes; Thermo Fisher Scientific, Inc.) at 1 or 24 h, as previously described (19,21). In brief, the cells were treated with 75 or 100 μM H_2O_2 with or without 10 μM MEK, JNK, or p38 inhibitor in the presence of 5 μM CMFDA. The CMF fluorescence was calculated using a FACStar flow cytometer (BD Biosciences) at 1 h. The CMF (GSH) levels were expressed as MFI, which was assessed by CellQuest Pro software (version 5.1; BD Biosciences). In addition, the cells were incubated with 75 or 100 μM H_2O_2 in the presence or absence of each MAPK inhibitor for 24 h. The CMF fluorescence intensity was measured by the FACStar flow cytometer (BD Biosciences). Negative CMF staining (GSH-depleted) cells were expressed as the percentage of cells. Similar to previous experiments (19,21), the CMF levels in the cells excluding GSH-depleted cells were expressed as MFI.

Statistical analysis. The results represent the mean of at least two independent experiments (mean ± SD). The Student's t-test or one-way ANOVA with post hoc analysis using Tukey's multiple comparison tests was used for parametric data. The results were considered statistically significant at P<0.05.

Results

MAPK inhibitors affect cell growth and death in H_2O_2-treated lung cancer cells. The cell growth and death effects of MAPK inhibitors (MEK, JNK and p38 inhibitors) were examined in H_2O_2-treated lung cancer cells. The same inhibitors were used to block MAPK signaling pathways in previous studies (19-21). After exposure to H_2O_2 for 24 h, the half maximal inhibitory concentration (IC50) in Calu-6 and A549 cells was ~50 and 100 μM based on MTT assay, respectively. In addition, H_2O_2 dose-dependently increased the number of Annexin V-FITC-positive Calu-6 and A549 cells (data not shown). Doses of 75 or 100 μM H_2O_2 were chosen to distinguish the differences in cell growth inhibition and death in each cell line in the presence or absence of each MAPK inhibitor. Treatment with 75 μM H_2O_2 caused ~60% growth inhibition in Calu-6 cells within 24 h (Fig. 1A). All MAPK inhibitors enhanced growth inhibition and JNK and p38 inhibitors

exhibited significant effects (Fig. 1A). Both MEK and JNK inhibitors significantly diminished the growth of Calu-6 control cells (Fig. 1A). Treatment with 75 μM H_2O_2 increased the percentage of the sub-G1 cells to ~20% (Fig. 2A and C). The MEK inhibitor exhibited a robust trend towards an increased number of sub-G1 cells in the H_2O_2-treated Calu-6 cells (Fig. 2A and C). Neither the JNK nor the p38 inhibitor significantly altered the numbers of the sub-G1 cells in these cells (Fig. 2A and C). In addition, the H_2O_2 treatment increased the percentage of Annexin V-FITC-positive stained Calu-6 cells (Fig. 2B and D). All the inhibitors increased the percentage of Annexin V-FITC-positive H_2O_2-treated Calu-6 cells (Fig. 2B and D).

Using another lung cancer cell line, the A549 cells, a 100 μM H_2O_2-treatment induced growth inhibition to ~50% within 24 h (Fig. 1B). None of the MAPK inhibitors significantly changed the growth of the H_2O_2-treated and untreated control cells (Fig. 1B). Treatment with 100 μM H_2O_2 alone increased the percentage of the sub-G1 cells to ~50% compared to the H_2O_2-untreated control cells (Fig. 3A and C). All inhibitors further augmented the percentage of the sub-G1 cells in the H_2O_2-treated cells (Fig. 3A and C), with the MEK inhibitor being the most potent. Furthermore, the H_2O_2 treatment increased the percentage of Annexin V-FITC-positive stained A549 cells (Fig. 3B and D). All inhibitors augmented the percentage of Annexin V-FITC-positive H_2O_2-treated cells (Fig. 3B and D), and both MEK and JNK inhibitors exhibited significant enhancement (Fig. 3B and D).

MAPK inhibitors influence MMP in H_2O_2-treated lung cancer cells. Cell death is closely correlated with the collapse of MMP (22). Thus, MMP in H_2O_2-treated Calu-6 and A549 cells was determined in the presence or absence of each MAPK inhibitor using Rhodamine 123 dye at 24 h. As expected, the loss of MMP was significantly detected in H_2O_2-treated Calu-6 cells (Fig. 4A and B). The MEK and p38 inhibitors slightly increased the loss of MMP in H_2O_2-treated Calu-6 cells, whereas the JNK inhibitor significantly boosted the loss of MMP (Fig. 4A and B). With regard to the MMP levels in lung cancer cells not including negative Rhodamine 123
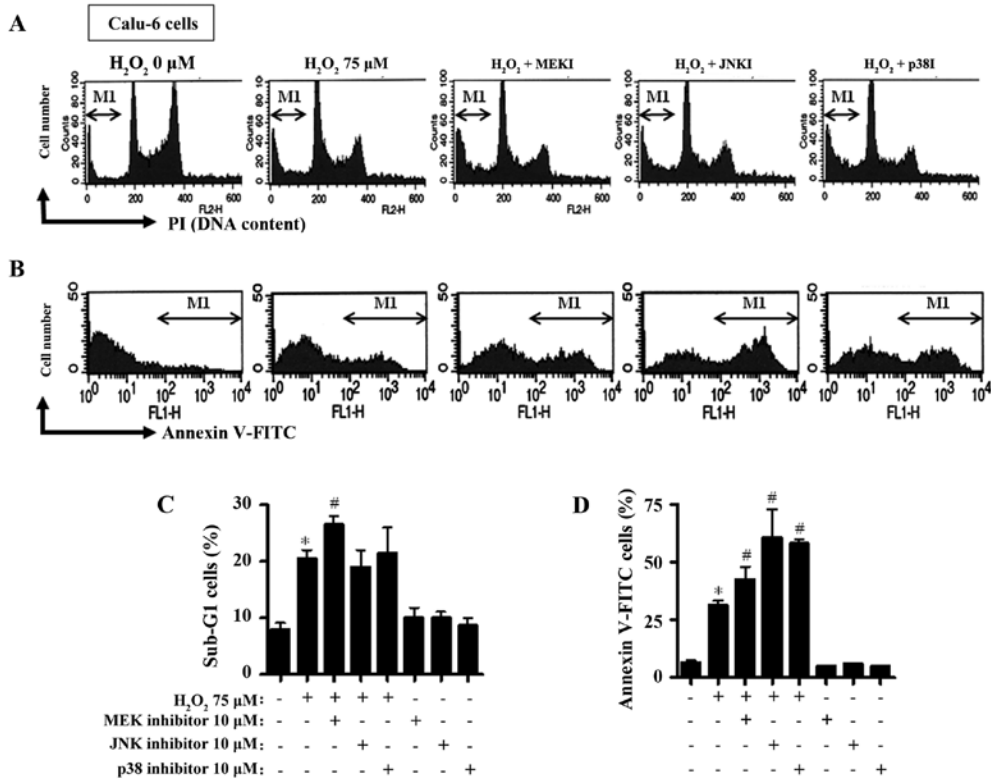
Figure 2. Effects of MAPK inhibitors on cell death in H$_2$O$_2$-treated Calu-6 cells. Followed by 30 min preincubation with the respective MAPK inhibitors, the exponentially growing Calu-6 cells were treated with 75 μM H$_2$O$_2$ for 24 h. (A) The images show representative cell cycle analysis, as analyzed by FACStar flow cytometer. M1 regions show sub-G1 cells. (B) The images show representative Annexin V-FITC staining cells, as analyzed by FACStar flow cytometer. M1 regions show Annexin V-FITC positive cells. (C and D) Graphs indicate the percentages of sub-G1 cells in M1 regions of (A) and Annexin V-FITC-positive cells in M1 regions of (B), respectively. *P<0.05 compared to the control group. #P<0.05 compared to cells treated only with H$_2$O$_2$.
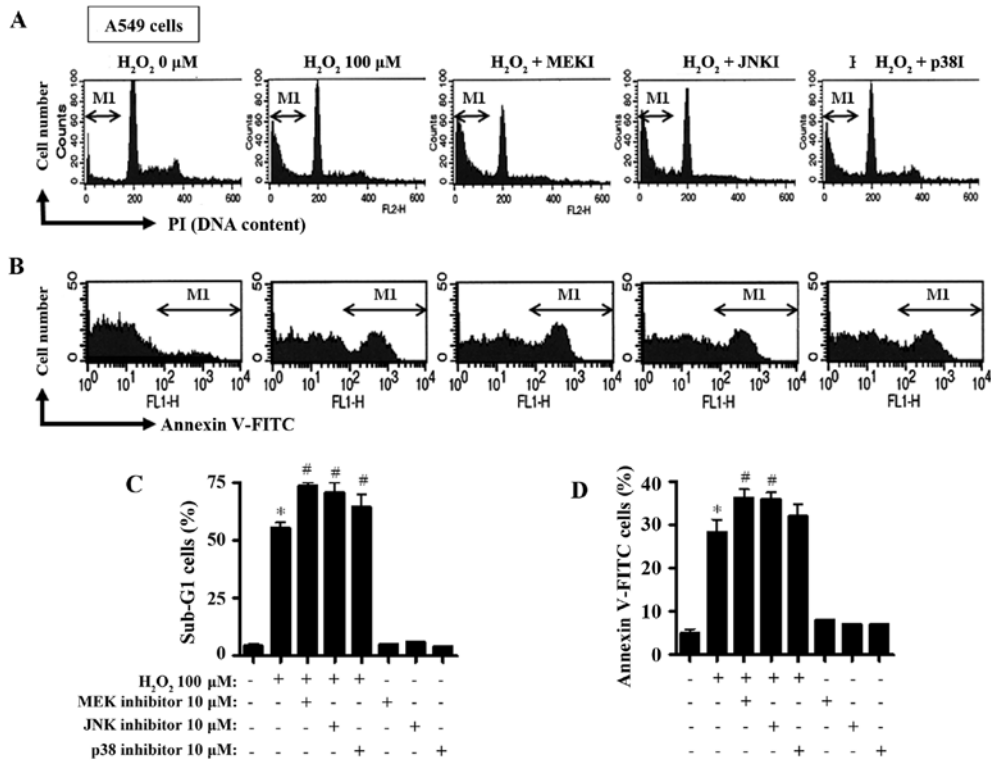
Figure 3. Effects of MAPK inhibitors on cell death in H$_2$O$_2$-treated A549 cells. After a 30 min preincubation with the respective MAPK inhibitors, exponentially growing A549 cells were treated with 100 μM H$_2$O$_2$ for 24 h. (A) The images show representative cell cycle analysis, as analyzed by FACStar flow cytometer. M1 regions show sub-G1 cells. (B) The images show representatives Annexin V-FITC staining cells, as analyzed by FACStar flow cytometer. M1 regions show Annexin V-FITC positive cells. (C and D) Graphs indicate the percentages of sub-G1 cells in M1 regions of (A) and Annexin V-FITC positive cells in M1 regions of (B), respectively. *P<0.05 compared to the control group. #P<0.05 compared to cells treated only with H$_2$O$_2$.
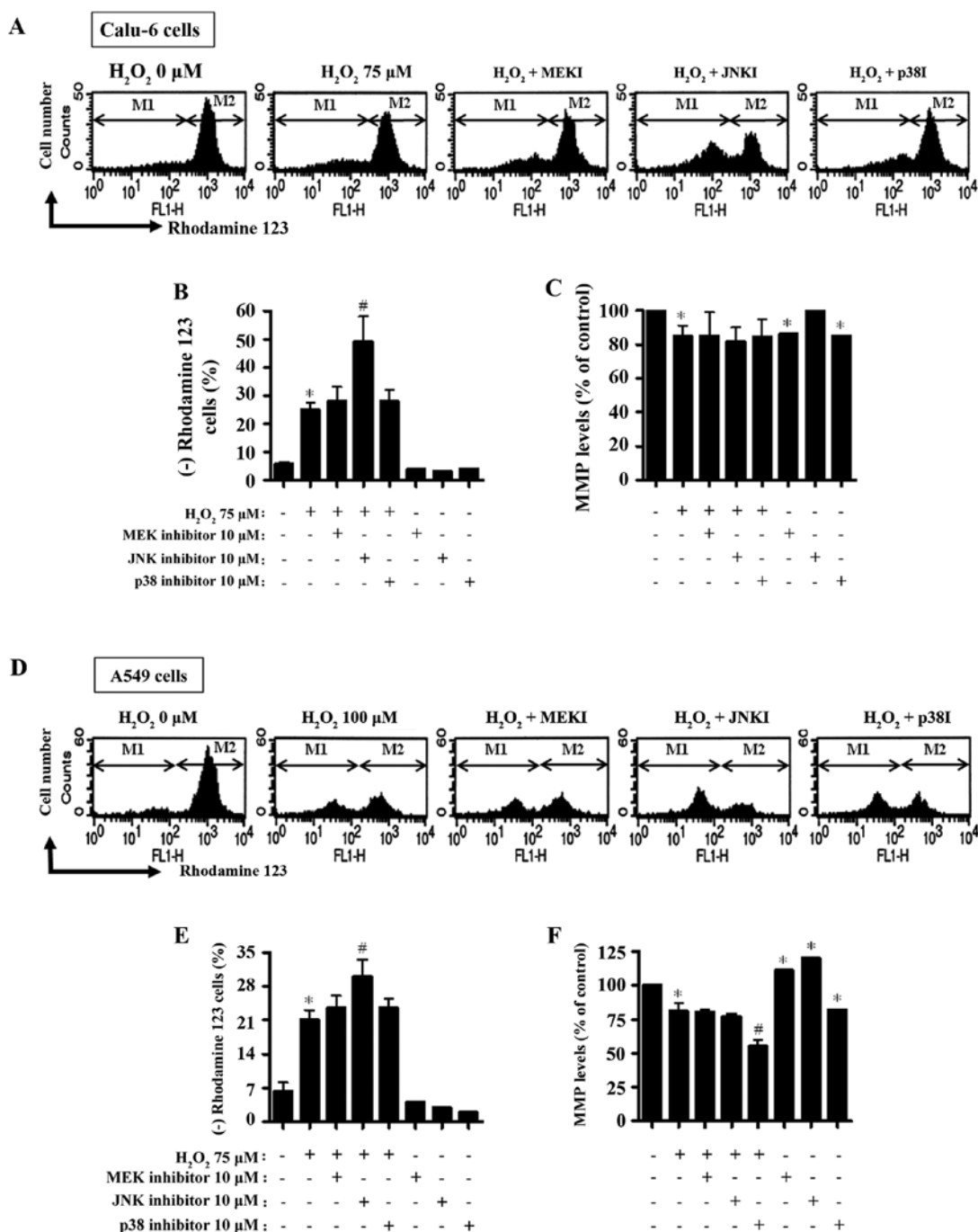
A

Calu-6 cells

B

H₂O₂ 75 µM:	-	+	+	+	+	-	-	-
MEK inhibitor 10 µM:	-	-	+	-	-	+	-	-
JNK inhibitor 10 µM:	-	-	-	+	-	-	+	-
p38 inhibitor 10 µM:	-	-	-	-	+	-	-	+

C

	-	+	+	+	+	-	-	-
	-	-	+	-	-	+	-	-
	-	-	-	+	-	-	+	-
	-	-	-	-	+	-	-	+

D

A549 cells

E

H₂O₂ 75 µM :	-	+	+	+	+	-	-	-
MEK inhibitor 10 µM :	-	-	+	-	-	+	-	-
JNK inhibitor 10 µM :	-	-	-	+	-	-	+	-
p38 inhibitor 10 µM :	-	-	-	-	+	-	-	+

F

	-	+	+	+	+	-	-	-
	-	-	+	-	-	+	-	-
	-	-	-	+	-	-	+	-
	-	-	-	-	+	-	-	+

Figure 4. Assessment of MMP in H_2O_2-treated lung cancer cells in the presence and absence of each MAPK inhibitor. Followed by 30-min preincubation with the respective MAPK inhibitors, exponentially growing lung cancer cells were treated with 75 or 100 μM H_2O_2 for 24 h. MMP in lung cancer cells was assessed by estimating incorporated Rhodamine 123 intensity using FACStar flow cytometer. (A and D) The images show the representative Rhodamine 123 staining of each cell line. M1 regions show Rhodamine 123-negative (MMP loss) cells in Calu-6 (A) and A549 cells (D). M2 regions show cells excluding MMP-loss cells. (B and E) Graphs show the percentage of Rhodamine 123-negative cells in M1 regions in Calu-6 (A) and A549 cells (D), respectively. (C and F) Graphs represent the percentages of mean MMP levels in M2 regions in Calu-6 (A) and A549 cells (D), respectively. *P<0.05 compared to the control group. #P<0.05 compared to cells treated only with H_2O_2.

staining cells, H_2O_2 decreased the MMP level in Calu-6 cells (Fig. 4A and C). None of the MAPK inhibitors influenced the MMP levels in H_2O_2-treated Calu-6 cells (Fig. 4A and C). The MEK and p38 inhibitors significantly reduced the MMP levels in Calu-6 control cells (Fig. 4A and C). Regarding the A549 cells, significant loss of MMP was observed in H_2O_2-treated cells (Fig. 4D and E). All inhibitors augmented the loss of MMP in H_2O_2-treated A549 cells and the JNK inhibitor

had a significant effect (Fig. 4D and F). While the MEK and JNK inhibitors did not alter the MMP levels in H_2O_2-treated A549 cells, the p38 inhibitor significantly enhanced the decrease in MMP levels in these cells (Fig. 4D and F). MEK and JNK inhibitors both significantly increased the MMP levels in H_2O_2-untreated A549 control cells, but the p38 inhibitor significantly decreased the MMP level in A549 control cells (Fig. 4D and F).
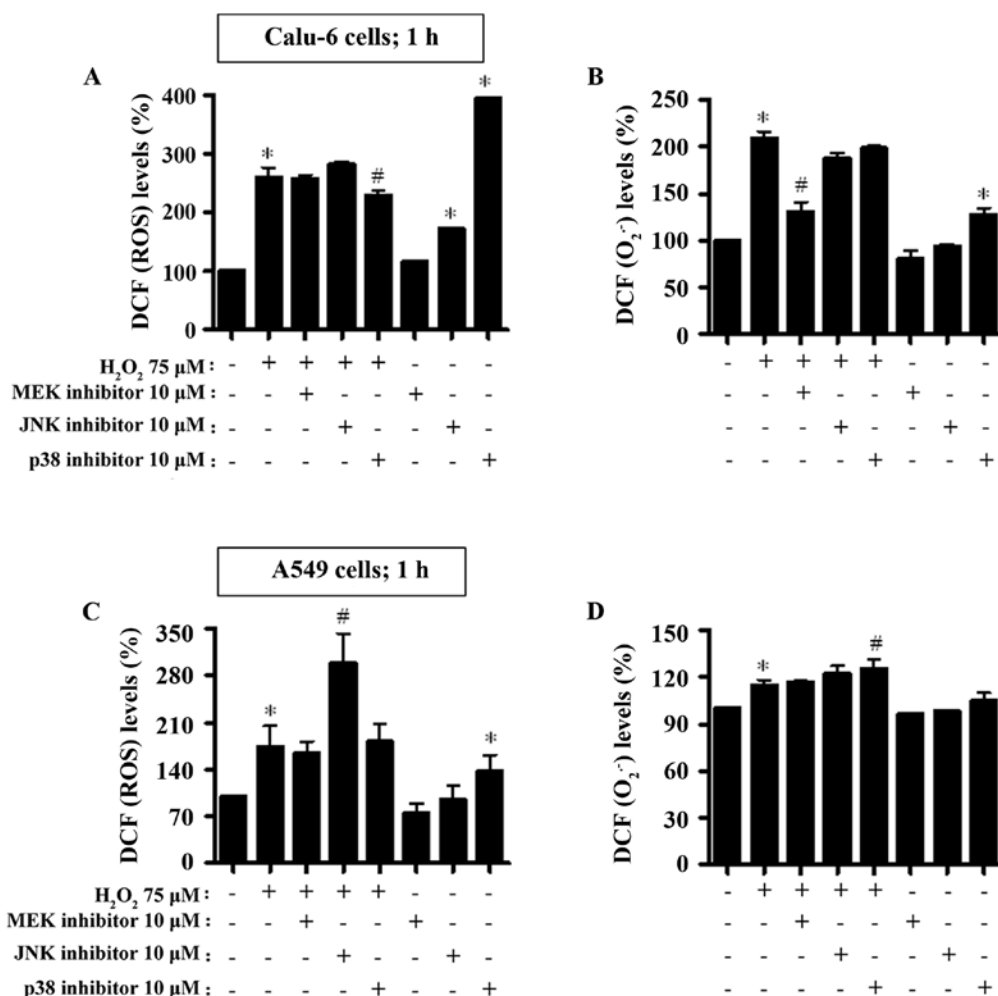
Figure 5. Effects of MAPK inhibitors on ROS levels in H$_2$O$_2$-treated lung cancer cells at 1 h. Exponentially growing cells were treated with 75 or 100 μM H$_2$O$_2$ for 1 h after 30 min of preincubation with the respective MAPK inhibitor. The ROS levels in lung cancer cells were assessed using a FACStar flow cytometer. (A and B) Graphs indicate DCF (ROS) and DHE (O$_2$$^{\cdot-}$) levels (%) in Calu-6 cells. (C and D) Graphs designate DCF (ROS) and DHE (O$_2$$^{\cdot-}$) levels (%) in A549 cells. *P<0.05 compared to the control group. $^#$P<0.05 compared to cells treated with H$_2$O$_2$ only.

MAPK inhibitors alter ROS levels including O$_2$$^{\cdot-}$ in H$_2$O$_2$-treated lung cancer cells. Changes in ROS levels were assessed in Calu-6 and A549 cells treated with H$_2$O$_2$ with or without each MAPK inhibitor. To determine whether the intracellular ROS levels in H$_2$O$_2$-treated lung cancer cells were altered by treatment with each MAPK inhibitor, ROS levels were assessed at the early time-point of 1 h (Fig. 5) and at the later time-point of 24 h (Fig. 6).

As depicted in Fig. 5A and C, intracellular ROS (DCF) levels were significantly increased in Calu-6 and A549 cells treated with H$_2$O$_2$ at 1 h. The JNK inhibitor increased the ROS (DCF) level in H$_2$O$_2$-treated Calu-6 cells, whereas the p38 inhibitor decreased the level in these cells (Fig. 5A). Both the JNK and p38 inhibitors significantly increased basal ROS (DCF) levels in Calu-6 control cells (Fig. 5A). In H$_2$O$_2$-treated A549 cells, the JNK inhibitor exhibited a strong significant increase in ROS (DCF) level (Fig. 5C). The MEK inhibitor decreased the basal ROS (DCF) level in A549 control cells, but the p38 inhibitor significantly increased the basal level (Fig. 5C). When the O$_2$$^{\cdot-}$ levels in H$_2$O$_2$-treated Calu-6 cells were assessed, the level of red fluorescence derived from DHE reflecting intracellular O$_2$$^{\cdot-}$ was significantly

increased (Fig. 5B). All MAPK inhibitors, especially the MEK inhibitor, exhibited a strong reduction of DHE (O$_2$$^{\cdot-}$) levels in H$_2O_2$-treated Calu-6 cells (Fig. 5B). In addition, the MEK inhibitor decreased the basal level of DHE (O$_2$$^{\cdot-}$) in Calu-6 control cells and the p38 inhibitor increased the basal level (Fig. 5B). Treatment with 100 μM H$_2$O$_2$ slightly increased DHE (O$_2$$^{\cdot-}$) levels in the A549 cells at 1 h (Fig. 5D). JNK and p38 inhibitors appeared to augment the DHE (O$_2$$^{\cdot-}$) levels in H$_2O_2$-treated A549 cells (Fig. 5D). The MEK and JNK inhibitors reduced basal levels in H$_2$O$_2$-untreated A549 control cells (Fig. 5D).

Treatment with 75 and 100 μM H$_2$O$_2$ increased the intracellular ROS (DCF and DHE) levels in Calu-6 and A549 cells at 24 h (Fig. 6). None of the MAPK inhibitors significantly affected ROS (DCF) levels in H$_2$O$_2$-treated Calu-6 and A549 cells (Fig. 6A and C). The JNK and p38 inhibitors increased ROS (DCF) levels in H$_2$O$_2$-untreated Calu-6 control cells (Fig. 6A), but both inhibitors decreased the levels in H$_2$O$_2$-untreated A549 control cells (Fig. 6C). Furthermore, the JNK and p38 inhibitors significantly augmented DHE (O$_2$$^{\cdot-}$) levels in H$_2O_2$-treated Calu-6 cells (Fig. 6B). All MAPK inhibitors increased the DHE (O$_2$$^{\cdot-}$) levels in H$_2O_2$-treated A549 cells (Fig. 6D).
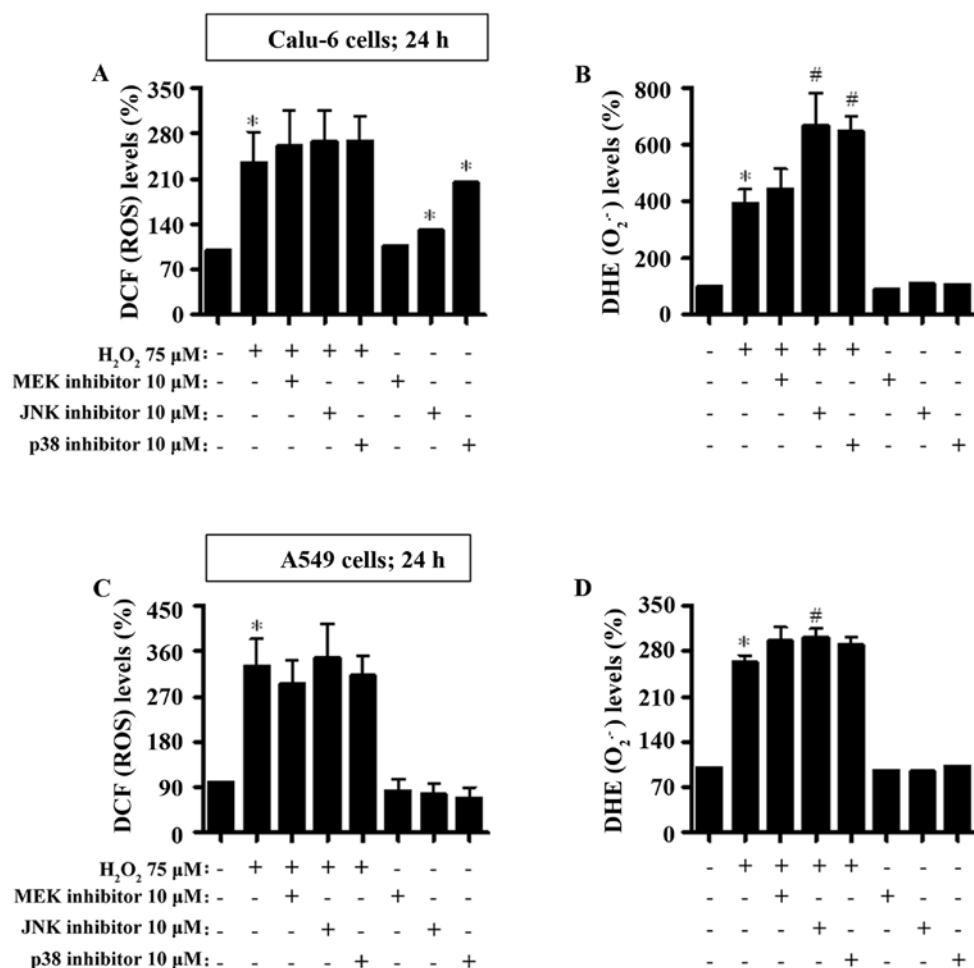
Figure 6. Measurement of ROS levels upon MAPK inhibitor pretreatment in H_2O_2-treated lung cancer cells at 24 h. Exponentially growing cells were treated with 75 or 100 μM H_2O_2 for 24 h after 30 min of preincubation with MAPK inhibitors. ROS levels, including $O_2^{\cdot-}$, were assessed in lung cancer cells using a FACStar flow cytometer. (A and B) The graphs indicate DCF (ROS) and DHE ($O_2^{\cdot-}$) levels (%) in Calu-6 cells. (C and D) The graphs show DCF (ROS) and DHE ($O_2^{\cdot-}$) levels (%) in A549 cells. *P<0.05 compared to the control group. #P<0.05 compared to cells treated with H_2O_2 only.
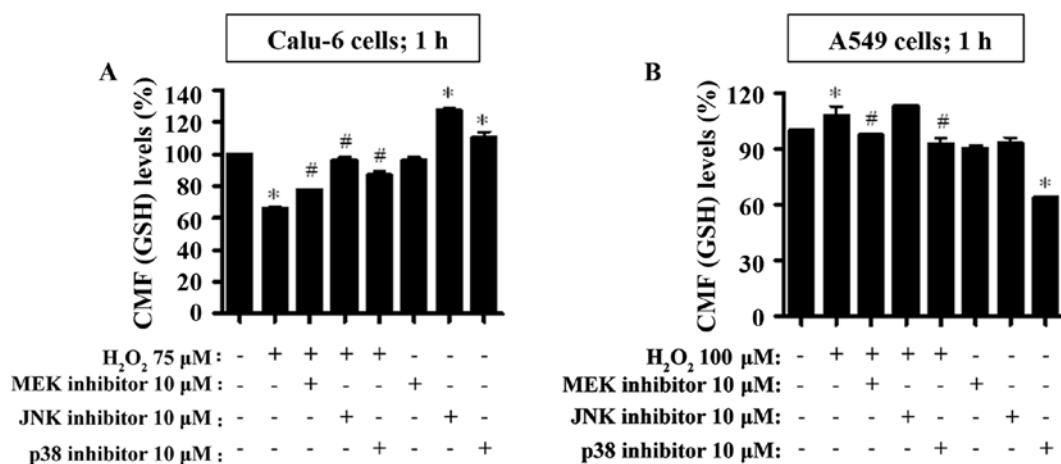

Figure 7. Estimation of GSH levels in H_2O_2-treated lung cancer cells prior to treatment with each MAPK inhibitor at 1 h. Exponentially growing cells were treated with 75 or 100 μM H_2O_2 for 1 h after 30 min of preincubation with MAPK inhibitors. GSH levels in lung cancer cells were calculated from the CMF intensity values obtained from FACStar flow cytometer analysis. (A and B) Graphs show the mean CMF (GSH) levels (%) in Calu-6 and A549 cells, respectively. *P<0.05 compared to the control group. #P<0.05 compared to cells treated only with H_2O_2.

MAPK inhibitors change GSH levels in H_2O_2-treated lung cancer cells. Changes in GSH levels were assessed in Calu-6 and A549 cells treated with H_2O_2 with or without each MAPK inhibitor at 1 h (Fig. 7) and at 24 h (Fig. 8). Treatment with 75 μM H_2O_2 strongly decreased the GSH levels in Calu-6 cells at 1 h (Fig. 7A). All MAKP inhibitors significantly increased
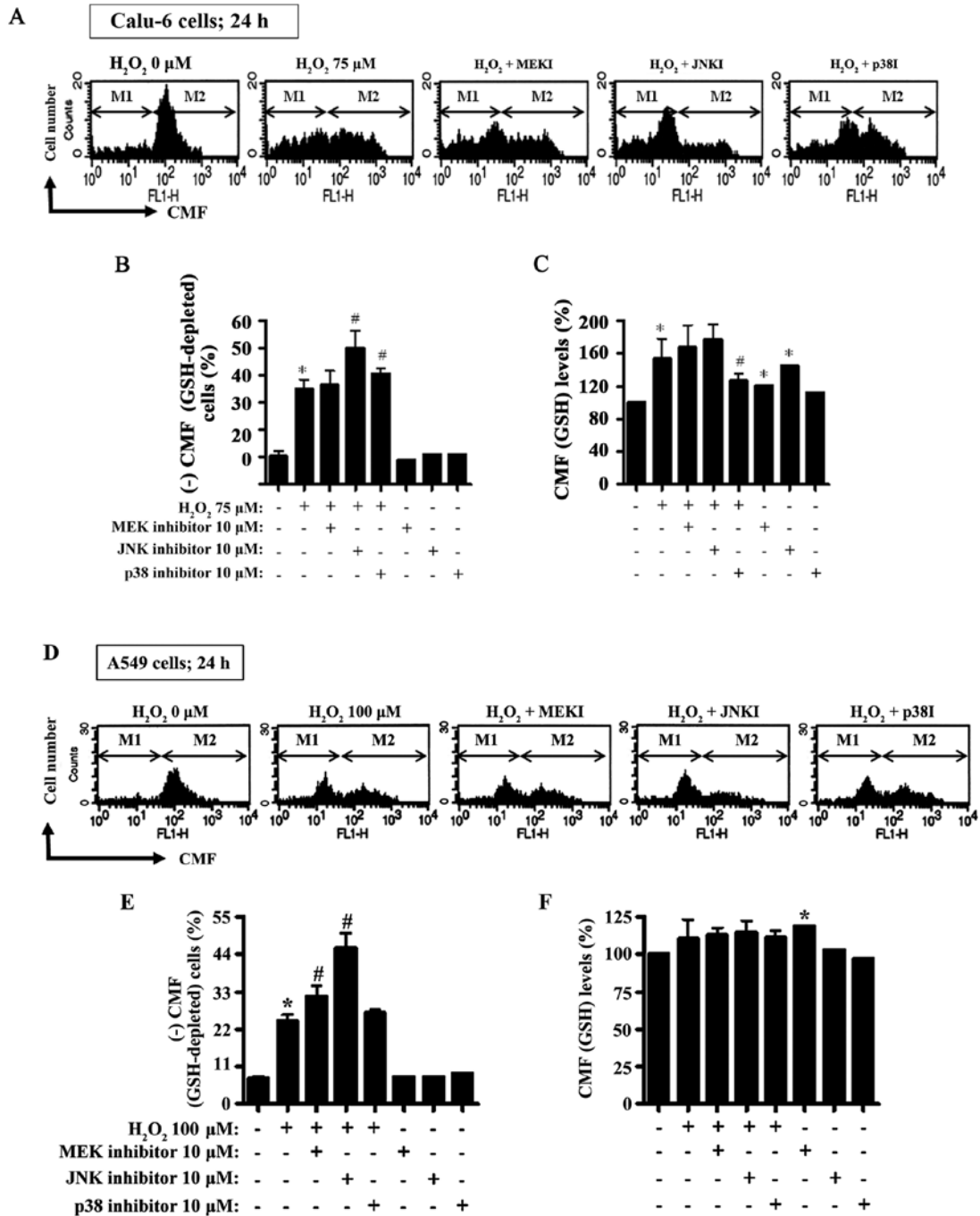
Figure 8. Evaluation of GSH levels in H$_2$O$_2$-treated lung cancer cells prior to treatment with MAPK inhibitors at 24 h. Exponentially growing cells were treated with 75 or 100 μM H$_2$O$_2$ for 24 h after 30 min preincubation with MAPK inhibitors. GSH levels in lung cancer cells were calculated from the CMF intensity values obtained from FACStar flow cytometer analysis. (A and D) The images demonstrate representative cells of each CMF-staining state. M1 regions illustrate CMF-negative stained (GSH-depleted) cells in Calu-6 (A) and A549 cells (D). M2 regions show cells excluding GSH-depleted cells. (B and E) Graphs show the percentage of Rhodamine 123-negative cells in M1 regions in Calu-6 (A) and A549 cells (D), respectively. (C and F) Graphs represent the percentages of mean CMF (GSH) levels in M2 regions in Calu-6 (A) and A549 cells (D), respectively. *P<0.05 compared to the control group. #P<0.05 compared to cells treated only with H$_2$O$_2$.

the GSH levels in the H$_2$O$_2$-treated Calu-6 cells (Fig. 7A). In addition, the JNK and p38 inhibitors augmented the basal levels of GSH in Calu-6 control cells (Fig. 7A). However, 100 μM H$_2$O$_2$ increased the GSH levels in A549 cells at 1 h (Fig. 7B). The MEK and p38 inhibitors attenuated the GSH levels in H$_2$O$_2$-treated A549 cells (Fig. 7B). All MAPK inhibitors decreased the GSH levels in H$_2$O$_2$-untreated A549 control cells and the decrease was more significant upon treatment with the p38 inhibitor (Fig. 7B).

Treatment with 75 μM H$_2$O$_2$ for 24 h resulted in an increase to ~25% in the GSH-depleted Calu-6 cells compared to the H$_2$O$_2$-untreated control cells (Fig. 8A and B). Unlike the MEK inhibitor, both the JNK and p38 inhibitors significantly increased GSH-depleted cell numbers in H$_2$O$_2$-treated Calu-6 cells (Fig. 8A and B). Furthermore, when the CMF (GSH) levels in Calu-6 cells (not including negative CMF-staining cells) were assessed at 24 h, the GSH levels exhibited an increase in H$_2$O$_2$-treated Calu-6 cells (Fig. 8A and C). Both the

MEK and JNK inhibitors did not significantly alter GSH levels in H_2O_2-treated Calu-6 cells, but the p38 inhibitor significantly attenuated the GSH level in these cells (Fig. 8A and C). All inhibitors increased the GSH levels in H_2O_2-untreated Calu-6 control cells and especially the JNK inhibitor expressed a strong increase (Fig. 8A and C). In relation to A549 cells, 100 μM H_2O_2 resulted in an increase in the number of GSH-depleted A549 cells to ~16% at 24 h compared to the H_2O_2-untreated control cells (Fig. 8D and E). The MEK and JNK inhibitors significantly enhanced the GSH deletion in H_2O_2-treated A549 cells (Fig. 8D and E). Treatment with 100 μM H_2O_2 did not significantly change the level of GSH at 24 h (Fig. 8D and F). None of the MAPK inhibitors altered the level of GSH in H_2O_2-treated A549 cells (Fig. 8D and F). The MEK inhibitor significantly increased the basal level of GSH in A549 control cells, whereas the p38 inhibitor reduced the level of GSH (Fig. 8D and F).

Discussion

Treatment with 75 and 100 μM H_2O_2 increased the number of sub-G1 and Annexin V-FITC-positive cells in Calu-6 and A549 lung cancer cells, accompanied by the downregulation of Bcl-2 and procaspase-3 proteins and activation of caspase-3 and -8 (data not shown). These results indicated that H_2O_2 induced cell death in these lung cancer lines via caspase-dependent apoptosis. The present study focused on evaluating the effects of MAPK inhibitors on cell growth and cell death as well as intracellular ROS and GSH levels in H_2O_2-treated lung cancer cells.

Usually, the ERK signaling pathway is pro-survival rather than pro-apoptotic (14). The MEK inhibitor, which presumably inactivates ERK, appeared to enhance growth inhibition in H_2O_2-treated Calu-6 cells. The MEK inhibitor significantly increased the number of sub-G1 and Annexin V-FITC-positive H_2O_2-treated Calu-6 and A549 cells. Thus, H_2O_2 seemed to inactivate ERK in lung cancer cells, resulting in growth inhibition and apoptosis. In most cases, the JNK and p38 activities are stimulated by ROS or a mild oxidative change in the intracellular thiol/disulfide redox condition, which is positively involved in the induction of apoptosis (11,12). However, both JNK and p38 inhibitors augmented the growth inhibition in H_2O_2-treated Calu-6 cells. In addition, both inhibitors significantly increased cell death in H_2O_2-treated Calu-6 and A549 cells. Therefore, in H_2O_2-treated lung cancer cells, the JNK and p38 signaling pathways are probably associated with cell growth or survival rather than cell death. Similar to these results, the JNK and p38 inhibitors enhanced the death of HeLa cervical cancer cells treated with 100 μM H_2O_2 (23). Interestingly, JNK and p38 inhibitors exhibited a significant increase in Annexin V-FITC-positive cells but did not increase the number of sub-G1 cells in H_2O_2-treated Calu-6 cells. Thus, the suppression of the JNK and p38 signaling pathways by each inhibitor induced necrotic cell death in H_2O_2-treated Calu-6 cells. In addition, none of the MAPK inhibitors significantly affected cell growth inhibition in H_2O_2-treated A549 cells, indicating that the MAPK signaling pathways are more associated with cell survival rather than cell growth. Furthermore, the MEK and JNK inhibitors reduced the growth of the Calu-6 control but not of the A549 control cells. These inhibitors differentially influenced the growth of Calu-6 and A549 lung cancer cells.

ROS can augment the disturbance of redox status in cells by triggering a breakdown in MMP (24). Correspondingly, H_2O_2 induced the loss of MMP in lung cancer cells. Similar to the percentage of Annexin V-FITC-positive cells, the JNK inhibitor strongly increased the loss of MMP in H_2O_2-treated lung cancer cells. However, the MEK and p38 inhibitors slightly enhanced the loss in these cells. These results indicated that JNK signaling is tightly involved in the maintenance of an intact MMP in lung cancer cells. The MMP levels in Rhodamine 123-positive cells revealed that H_2O_2 reduced the MMP levels in lung cancer cells. Only the p38 inhibitor enhanced a decrease in MMP levels in H_2O_2-treated A549 cells. In addition, the MEK inhibitor decreased the basal MMP level in H_2O_2-untreated Calu-6 cells but increased the basal level in A549 control cells. The JNK inhibitor increased the basal MMP level in H_2O_2-untreated A549 cells. The p38 inhibitor reduced the basal MMP levels in both Calu-6 and A549 control cells. These results indicated that each MAPK signaling pathway had different and specific effects on MMP in Calu-6 and A549 lung cancer cells.

The main ROS related to cell signaling pathways are $O_2^{\cdot-}$ and H_2O_2. Intracellular ROS levels, including $O_2^{\cdot-}$, were significantly increased in both lung cancer cells treated with H_2O_2 at 1 and 24 h. Treatment with 75 and 100 μM H_2O_2 directly produced $O_2^{\cdot-}$ by impairing the mitochondrial membrane function and both H_2O_2 and $O_2^{\cdot-}$ can be efficiently converted into toxic $\cdot$OH via the Fenton reaction to destroy these cancer cells. However, H_2O_2 slightly increased $O_2^{\cdot-}$ (DHE) levels in A549 cells compared to Calu-6 cells at 1 h, indicating that it does not have a strong effect on both mitochondrial respiratory transport chain and the activity of various oxidases to generate $O_2^{\cdot-}$ in A549 cells within this early time-point. Only the JNK inhibitor significantly enhanced the increased ROS (DCF) levels in H_2O_2-treated Calu-6 and A549 cells at 1 h. Both JNK and p38 inhibitors increased $O_2^{\cdot-}$ (DHE) levels in H_2O_2-treated A549 cells at 1 h. In contrast, the MEK inhibitor decreased $O_2^{\cdot-}$ (DHE) levels in H_2O_2-treated Calu-6 cells at 1 h and the p38 inhibitor decreased ROS (DCF) levels in these cells at 1 h. In addition, none of the MAPK inhibitors significantly altered ROS (DCF) levels in H_2O_2-treated lung cancer cells at 24 h. However, all MAPK inhibitors, especially the JNK and p38 inhibitors augmented DHE ($O_2^{\cdot-}$) levels in H_2O_2-treated Calu-6 and A549 cells at 24 h. Thus, it is plausible that the enhancement of H_2O_2-induced lung cancer cell death by MAPK inhibitors, especially the JNK inhibitor, is more related to the levels of $O_2^{\cdot-}$ (DHE) rather than ROS (DCF). Furthermore, although the JNK and p38 inhibitors significantly increased ROS (DCF) levels in Calu-6 control cells at 1 and 24 h, these inhibitors did not significantly provoke cell death and MMP loss. Additionally, each MAPK inhibitor had different effects on basal ROS (DCF) and $O_2^{\cdot-}$ (DHE) levels in H_2O_2-untreated Calu-6 and A549 control cells regardless of cell death. Since changes in $O_2^{\cdot-}$ and H_2O_2 levels by these MAPK inhibitors and the outcomes of their corresponding signaling pathways influenced by these types of ROS are complex in cells and different in each cell type, the detailed molecular mechanisms underlying the effects of MAPK inhibitors and their relationship between ROS and cell death require further study.

GSH is an important tripeptide (non-protein) antioxidant in cells. GSH content has a vital effect on cell death (25-27). Similarly, H_2O_2 increased the percentage of GSH-depleted cells in both Calu-6 and A549 lung cancer cells at 24 h. In addition, the JNK inhibitor effects of enhancing cell death and MMP loss in H_2O_2-treated lung cancer cells significantly increased the number of GSH-depleted cells in these cells. Additionally, the p38 inhibitor augmented GSH depletion in H_2O_2-treated Calu-6 cells and the MEK inhibitor enhanced the depletion in H_2O_2-treated A549 cells. These results supported the hypothesis that cell death effects are inversely proportional to GSH content (26,28,29). However, the MEK inhibitor did not increase GSH depletion in H_2O_2-treated Calu-6 cells and the p38 inhibitor did not enhance GSH depletion in H_2O_2-treated A549 cells. Therefore, the loss of GSH content is necessary, but not sufficient for the accurate prediction of cell death in lung cancer cells. JNK signaling, among other MAPK signaling pathways, appeared to be more significant for the relationship between cell death and GSH depletion. H_2O_2 decreased CMF (GSH) levels in Calu-6 cells at 1 h, probably as a result of its use to scavenge intracellular ROS. All MAPK inhibitors, especially the JNK and p38 inhibitors, increased GSH levels in H_2O_2-treated and untreated Calu-6 cells at 1 h, indicating that these inhibitors positively preserved GSH content in Calu-6 cells. However, 75 μM H_2O_2 increased CMF (GSH) levels in Calu-6 cells excluding GSH-depleted cells at 24 h. It is likely that this increase was required to reduce the intracellular ROS levels increased by H_2O_2 to protect cells from immediate cell death. The p38 inhibitor significantly diminished GSH levels in H_2O_2-treated Calu-6 cells at 24 h. Both the MEK and JNK inhibitors raised the basal levels of GSH in H_2O_2-treated Calu-6 cells at 24 h. In addition, 100 μM H_2O_2 did not significantly alter GSH levels in A549 cells at 1 and 24 h. MEK and p38 inhibitors reduced GSH in H_2O_2-treated A549 cells at 1 h. All MAPK inhibitors, especially the p38 inhibitor, reduced the basal levels of GSH in A549 control cells at 1 h. None of the MAPK inhibitors influenced GSH levels in H_2O_2-treated A549 cells at 24 h. However, the MEK inhibitor increased basal GSH levels in A549 control cells at 24 h. Consequently, these results revealed that each MAPK signaling pathway differently influences intracellular GSH levels irrespective of GSH-depleted cells dependent on cell types, incubation times and the presence or absence of H_2O_2. The exact functions of each MAPK inhibitor in H_2O_2-induced lung cell death still need to be further defined with respect to changes in ROS and GSH.

In conclusion, exogenous H_2O_2 induced growth inhibition and cell death in Calu-6 and A549 lung cancer cells by increasing intracellular ROS and depleting GSH. All MAPK inhibitors generally amplified H_2O_2-induced lung cancer cell death. Especially, the enhanced cell death and MMP loss effects of the JNK inhibitor in H_2O_2-treated lung cancer cells were related to increased $O_2^{\cdot-}$ (DHE) levels and GSH depletion.

Acknowledgements

References

1. Gonzalez C, Sanz-Alfayate G, Agapito MT, Gomez-Niño A, Rocher A and Obeso A: Significance of ROS in oxygen sensing in cell systems with sensitivity to physiological hypoxia. Respir Physiol Neurobiol 132: 17-41, 2002.
2. Baran CP, Zeigler MM, Tridandapani S and Marsh CB: The role of ROS and RNS in regulating life and death of blood monocytes. Curr Pharm Des 10: 855-866, 2004.
3. Zorov DB, Juhaszova M and Sollott SJ: Mitochondrial ROS-induced ROS release: An update and review. Biochim Biophys Acta 1757: 509-517, 2006.
4. Zelko IN, Mariani TJ and Folz RJ: Superoxide dismutase multigene family: A comparison of the CuZn-SOD (SOD1), Mn-SOD (SOD2), and EC-SOD (SOD3) gene structures, evolution, and expression. Free Radic Biol Med 33: 337-349, 2002.
5. Wilcox CS: Reactive oxygen species: Roles in blood pressure and kidney function. Curr Hypertens Rep 4: 160-166, 2002.
6. Blaser H, Dostert C, Mak TW and Brenner D: TNF and ROS crosstalk in inflammation. Trends Cell Biol 26: 249-261, 2016.
7. Reuter S, Gupta SC, Chaturvedi MM and Aggarwal BB: Oxidative stress, inflammation, and cancer: How are they linked? Free Radic Biol Med 49: 1603-1616, 2010.
8. Genestra M: Oxyl radicals, redox-sensitive signalling cascades and antioxidants. Cell Signal 19: 1807-1819, 2007.
9. Kusuhara M, Takahashi E, Peterson TE, Abe J, Ishida M, Han J, Ulevitch R and Berk BC: p38 Kinase is a negative regulator of angiotensin II signal transduction in vascular smooth muscle cells: Effects on Na⁺/H⁺ exchange and ERK1/2. Circ Res 83: 824-831, 1998.
10. Blenis J: Signal transduction via the MAP kinases: Proceed at your own RSK. Proc Natl Acad Sci USA 90: 5889-5892, 1993.
11. Hsin YH, Chen CF, Huang S, Shih TS, Lai PS and Chueh PJ: The apoptotic effect of nanosilver is mediated by a ROS- and JNK-dependent mechanism involving the mitochondrial pathway in NIH3T3 cells. Toxicol Lett 179: 130-139, 2008.
12. Mao X, Yu CR, Li WH and Li WX: Induction of apoptosis by shikonin through a ROS/JNK-mediated process in Bcr/Abl-positive chronic myelogenous leukemia (CML) cells. Cell Res 18: 879-888, 2008.
13. Guyton KZ, Liu Y, Gorospe M, Xu Q and Holbrook NJ: Activation of mitogen-activated protein kinase by H_2O_2. Role in cell survival following oxidant injury. J Biol Chem 271: 4138-4142, 1996.
14. Henson ES and Gibson SB: Surviving cell death through epidermal growth factor (EGF) signal transduction pathways: Implications for cancer therapy. Cell Signal 18: 2089-2097, 2006.
15. Latimer HR and Veal EA: Peroxiredoxins in regulation of MAPK signalling pathways; Sensors and barriers to signal transduction. Mol Cells 39: 40-45, 2016.
16. Rhee SG, Kang SW, Jeong W, Chang TS, Yang KS and Woo HA: Intracellular messenger function of hydrogen peroxide and its regulation by peroxiredoxins. Curr Opin Cell Biol 17: 183-189, 2005.
17. Vilhardt F and van Deurs B: The phagocyte NADPH oxidase depends on cholesterol-enriched membrane microdomains for assembly. EMBO J 23: 739-748, 2004.
18. Hinz B, Phan SH, Thannickal VJ, Prunotto M, Desmoulière A, Varga J, De Wever O, Mareel M and Gabbiani G: Recent developments in myofibroblast biology: Paradigms for connective tissue remodeling. Am J Pathol 180: 1340-1355, 2012.
19. Han YH and Park WH: The effects of MAPK inhibitors on a proteasome inhibitor, MG132-induced HeLa cell death in relation to reactive oxygen species and glutathione. Toxicol Lett 192: 134-140, 2010.
20. Han YH and Park WH: Pyrogallol-induced As4.1 juxtaglomerular cell death is attenuated by MAPK inhibitors via preventing GSH depletion. Arch Toxicol 84: 631-640, 2010.
21. Han YH, Moon HJ, You BR and Park WH: The effects of MAPK inhibitors on pyrogallol-treated Calu-6 lung cancer cells in relation to cell growth, reactive oxygen species and glutathione. Food Chem Toxicol 48: 271-276, 2010.
22. Yang J, Liu X, Bhalla K, Kim CN, Ibrado AM, Cai J, Peng TI, Jones DP and Wang X: Prevention of apoptosis by Bcl-2: Release of cytochrome c from mitochondria blocked. Science 275: 1129-1132, 1997.
23. Park WH: The effect of MAPK inhibitors and ROS modulators on cell growth and death of H_2O_2-treated HeLa cells. Mol Med Rep 8: 557-564, 2013.

24. Campo ML, Kinnally KW and Tedeschi H: The effect of antimycin A on mouse liver inner mitochondrial membrane channel activity. J Biol Chem 267: 8123-8127, 1992.
25. Han YH, Kim SH, Kim SZ and Park WH: Carbonyl cyanide *p*-(trifluoromethoxy) phenylhydrazone (FCCP) as an $O_2(*-)$ generator induces apoptosis via the depletion of intracellular GSH contents in Calu-6 cells. Lung Cancer 63: 201-209, 2009.
26. Estrela JM, Ortega A and Obrador E: Glutathione in cancer biology and therapy. Crit Rev Clin Lab Sci 43: 143-181, 2006.
27. Han YH, Kim SZ, Kim SH and Park WH: Intracellular GSH level is a factor in As4.1 juxtaglomerular cell death by arsenic trioxide. J Cell Biochem 104: 995-1009, 2008.
28. Han YH, Kim SZ, Kim SH and Park WH: Enhancement of arsenic trioxide-induced apoptosis in HeLa cells by diethyl-dithiocarbamate or buthionine sulfoximine. Int J Oncol 33: 205-213, 2008.
29. Han YH, Kim SZ, Kim SH and Park WH: Suppression of arsenic trioxide-induced apoptosis in HeLa cells by N-acetylcysteine. Mol Cells 26: 18-25, 2008.